2012 14th International Conference on Ground Penetrating Radar (GPR)
June 4-8, 2012, Shanghai, China @ ISBN 978-1-4673-2663-6

3D Segmentation of Ground Penetrating Radar Data for Landmine Detection

Dyana A, CH Srinivas Rao and Ramachandra Kuloor
Electronics and Radar Development Establishment
Defence Research and Development Organisation
Bangalore- 560 093, India
dyana.a@lrde.drdo.in, srinivas.rao.ch@lrde.drdo.in, kuloor@lrde.drdo.in

Abstract — **In this paper, we propose a 3D image analysis method for landmine detection from vehicle mounted Ground Penetrating Radar (GPR) data, using adaptive filtering technique and image segmentation algorithm. Conventional methods for landmine detection seldom exploit the 3D information (C-Scan) and the discrimination algorithms used are computationally expensive. In our method, we have used 3D adaptive filtering technique (3D LMS), which is suitable for real-time applications for locating the anomalies in C-Scan data. Gradient Vector Flow Deformable Model based segmentation algorithm is applied on the localized regions to obtain a 3D volumetric segmented image. The segmented regions' shape features are used to further discriminate targets from clutters to obtain a 3D segmented image of landmines. Data collected from 3D Radar system and Vector Network Analyzer (VNA) based SFCW-GPR is used for performance evaluation of the proposed algorithm. Our proposed method has shown better performance than other state-of-the-art algorithms for landmine detection, in terms of its Receiver Operating Characteristic (ROC) measure.**

Keywords- Vehicle Mounted GPR, C Scan Data, 3D Least Mean Square Algorithm, Segmentation, Gradient Vector Flow Snakes, Landmine Detection, 3D image analysis

I. Introduction

Landmine detection is imperative for the purpose of military applications and humanitarian demining. The technologies developed for landmine detection [1] includes Electromagnetic induction (EMI), Ground Penetrating radar (GPR) [2] [8], Radiometer, Nuclear Quadrupole resonance, Neutron based methods, Acoustic sensors etc. Ground Penetrating Radar, when mounted on vehicle, is used to image the subsurface in 3D (x, y and z), termed as C-scan data. Clutter is the major factor that limits the detectability of landmines. Clutter is caused not only by inhomogeneities in the soil and its topological variations but also by various deterministic reflectors, such as small metal fragments, shrapnel, spent bullet and cartridge cases, puddles of water, tufts of grass, animal burrows, cracks and fissures in the ground, rocks, and stones.

The simplest detection technique is peak energy detection, where all energy over each GPR profile is integrated over the profile and projected on the ground surface. This approach works well only for the detection of strong subsurface reflectors, as weak reflections are masked by the surface clutter. Hyperbola [18] and Ellipse detection algorithms are applied on images or slices of GPR data to detect anomalies. However, inhomogeneity of the ground results in a shape other than a hyperbola for the reflector response. Different statistical tests can be applied to B-scans (or C-scans) to detect variations from the background models including Kalman filter [19], Particle Filter [10] , generalized likelihood ratio [6] , fuzzy logic [5], and abrupt change detection theory [12]. Least Mean Square (LMS) algorithm [19] is widely used for anomaly detection from vehicle mounted GPR data due to its simplicity and applicable for real-time situations. In this paper, we refer the LMS used for landmine detection by Torrione et al. [11], as 2D-LMS. In our work, we have improved the performance of 2D LMS for anomaly detection, by processing the 3D data from three different planes.

Migration techniques are used for imaging the GPR data [4]. Intensity based segmentation algorithms are applied on migrated GPR data [16] Migration algorithms are computationally expensive and prior knowledge of permittivity of soil is required for perfect imaging of data. Low level image segmentation algorithms may generate infeasible object boundaries as it extracts only local information. In this paper, we have used deformable model based image segmentation algorithm to get object boundaries, which could accommodate significant variations in target structure.

In our work, the data is first preprocessed by applying mean based clutter removal algorithm and median filter to remove clutter/noise. After clutter reduction, each point in the 3D data is predicted from its neighborhood by applying adaptive filter technique called 3D LMS algorithm, which we have proposed in [3], to identify potential location of targets. Gradient Vector Flow Deformable model based algorithm is applied on identified volumes of interest (potential target locations) to segment objects from background. The segmented regions properties are used to discriminated targets from clutter. The organization of the paper is as follows. Our proposed system is discussed in detail in Section II. Experimental results are presented and discussed in Section III and Section 1V concludes the paper.

II. Proposed Landmine Detection Algorithm

The data collected by GPR is of three dimensional (cross track (x), down track (y) and time/depth (z)). The raw time domain data is composed of clutter, noise and targets. Hence the raw data is first preprocessed to accentuate the targets and reduce clutter/noise. Discrimination algorithms for landmine detection are computationally expensive. Hence we use anomaly detector to locate volumes of interest. Discrimination algorithm is then applied only on the identified volumes. To detect anomalies from the preprocessed data, we have used 3D Least Mean Square Algorithm, proposed by us in [3]. Gradient Vector Flow Deformable Model is used for locating object boundaries of the detected anomalies, to get 3D volumetric segmented image. Solidity of the segmented region is used as a feature to discriminate targets from clutters.

A. Preprocess

The 3D GPR data is first preprocessed to remove the ground bounce caused due to air - ground interface. The first few time samples which consist of air to ground reflection and last few samples which have low signal to noise ratio is clipped off and not included for further processing. The number of time samples to ignore is chosen conservatively, so as to preserve the shallow buried targets. A sample volume of time-domain clipped data is shown in Fig. 1a. The next step is to remove the clutter caused due to antenna leakage and other background features. Mean based ground removal [13] is applied for each channel separately to remove the clutter. The data also consists of artefacts caused due to the interference from communication networks. Median filter is used to reduce this artefact. Preprocessed data is shown in Fig. 1b for the input data shown in Fig. 1a.

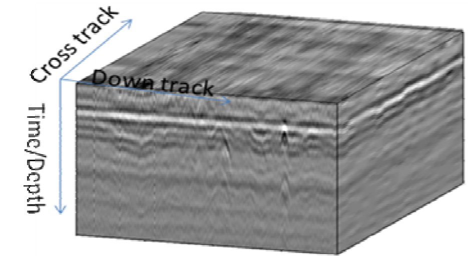

(a)

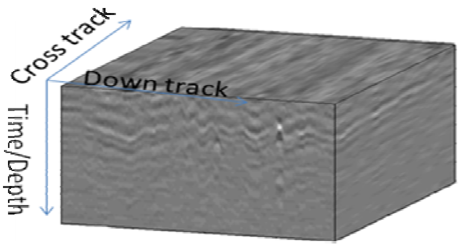

(b)

Figure 1. (a) Raw Data (b) Preprocessed data

After preprocessing, the targets get accentuated and anomaly detection algorithm is applied on the pre-processed data to locate volumes of interest, as discussed in the following subsection.

B. 3D Anomaly Detection

LMS algorithm uses gradient descent method to estimate a time varying signal and is suitable for real-time applications. We have used this technique as a prescreener for landmine detection in GPR. LMS is applied on three different slices obtained from the 3D cube to predict a voxel. Hence, we have termed the algorithm as three dimensional Least Mean Square Algorithm (3D LMS).

The object of interest (landmine) occupies a small volume of data in the C-scan (3D) data, collected by ground penetrating radar mounted on a vehicle. The algorithm works on the assumption that the clutter is correlated and occupies a large volume in the 3D cube, while the target occupies a small volume. Input to the LMS algorithm is a vector of pixels obtained from the neighborhood of the point of interest. The LMS algorithm is an adaptive filtering technique and the filter weights adapts to the clutter, as it adjusts its weights according to the time varying inputs. The filter weights are used to predict the successive point of interest. The difference between the predicted value from the LMS and the desired (actual) value gives the error in prediction. The same process is applied on three different planes for a point of interest. The three prediction errors are then fused to detect the anomaly.

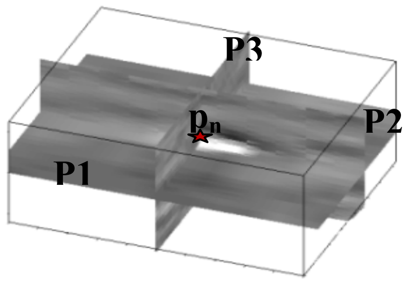

(a)

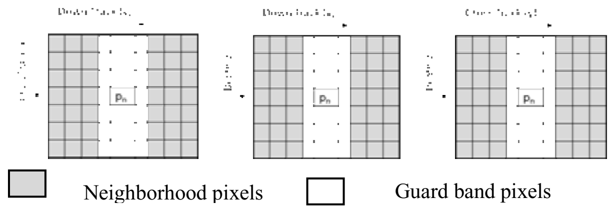

(b)

Figure 2. (a) Processing planes for 3D LMS for the point of interest marked at the centre. (b) Processing Window on the three planes (P1, P2, P3 from left to right) to predict a point of interest (pn). The window is not shown to scale.

Consider a point of interest p_n in a particular depth slice, at a time instant *n* and a plane (P1) as shown in Fig. 2a. The neighboring pixels which lie on the plane P1 is chosen from the window as shown in Fig 2b. Vector x_n is formed from these neighborhood pixels for the point p_n. Guard band distance is considered such that the target pixels are not included for estimating the point. Weight vector w_n is initialized with random values. The prediction value y_n is computed using the following equation.

$$y_n = w_n^t * x_n \tag{1}$$

The difference between the desired point and the predicted point gives the prediction error e_{1n} (Eqn. 2).

$$e_{1n} = y_n - p_n \tag{2}$$

The weight vector is adjusted using the following equation

$$w_{n+1} = w_n + \mu * x_n * e_{1n} \tag{3}$$

where, μ is the learning rate. The prediction error (e_{1n}) is used to obtain the decision statistic for the presence of target.

Similarly LMS is applied on the other two planes P2 and P3 and prediction errors are estimated from the neighbouring pixels (Fig. 2b). If e_{1n}, e_{2n} and e_{3n} are the three prediction errors by processing on three planes P1, P2 and P3 respectively for a point of interest p_n, the final prediction error for the point p_n is given by the weighted summation as follows:

$$e_n = w_{e1} * e_{1n} + w_{e2} * e_{2n} + w_{e3} * e_{3n} \tag{4}$$

The optimal values for w_{e1}, w_{e2} and w_{e3} in Eqn. 4 are found empirically from the performance of algorithm over a set of collected data (offline), for different values of weights. In real-time, the computed optimal values could be used. The prediction error (e_n) gives the final decision statistic for the presence of anomaly. Higher the prediction error, higher is the confidence for the presence of target and vice versa.

In 3D LMS, a voxel is estimated from the spatially correlated clutter in all three dimensions. This combined decision statistic increases the performance of 2D LMS applied on GPR data. The clutter characteristics vary in three different planes (xy, yz and xz) and they are spatially correlated within the plane. Hence we have applied three LMS filters to predict a voxel in the 3D cube. The loss of energy in z direction is also taken care by applying LMS on every depth plane separately. The individual LMS filters can be implemented in parallel and hence can be efficiently used for real-time applications.

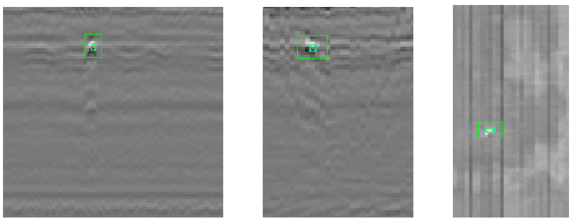

(a) (b) (c)

Figure 3. Detections from the 3D LMS Algorithm shown as marked rectangles on three different views: (a) Inline view (depth vs. Downtrack) (b) Bscan view (depth vs. cross track) (c) Top view (inline vs crosstrack).

To apply a common threshold for the decision statistic (e), adaptive whitening technique is implemented. This process is used to mitigate the effects caused due to loss of energy in the depth dimension. The whitening equation is given below:

$$d_w = \frac{e_n - \mu}{\sigma} \tag{5}$$

where, μ and σ are the mean and standard deviation of decision statistics of the neighboring pixels in xy plane for the point of interest p_n. To localize the detected object in correct position and to find the size of the object, morphological operations are applied on the whitened decision statistics (d_w). The decision statistic is thresholded and then dilated. The dilated regions are labeled based on the connectivity of voxels. Bounding area of the region is computed to find the potential area of the target. Figure 3 shows the detected targets using 3D LMS algorithm. The bounding area of the target is shown in three different views. 3D LMS gives the bounding area of the anomaly, thereby reducing the size of data to be processed by classification algorithms.

C. 3D Segmentation

The volumes of interest (potential location of targets) are identified by the anomaly detection algorithm discussed in the previous section. The volumes of interest are then segmented to obtain a 3D volumetric segmented image. Low level image segmentation algorithms such as edge detection, region growing algorithms consider only local information and cause infeasible object boundaries. 'Snakes' [7] are planar deformable contours which approximates the shape of objects based on the assumption that object boundaries are piecewise continuous or smooth. We have used Gradient Vector Flow (GVF) Snakes for locating object boundaries, as it converges to boundary concavities and they do not need to be initialized close to the boundary. The algorithm is applied on the envelope of data, obtained using Hilbert transform of A-scan time domain data.

GVF Snakes are applied independently on the potential target regions sliced from the identified volume. Snake contour is initialized with a rectangle which encloses the bounding box of identified region (crosstrack vs downtrack).

GVF Snake contour is represented as a time varying parametric contour by,

$$v(s,t) = (x(s,t), y(s,t)) \tag{6}$$

where x and y are the cross track and down track co-ordinates respectively. Dynamic GVF snake equation is given by,

$$v(s,t) = av''(s,t) - \beta v''''(s,t) + g \tag{7}$$

where first two terms dictates the internal forces (stretching and bending) of snake and last term is the external image force given by the gradient vector flow. Gradient vector flow field (g) is computed as given in [17]. GVF snake is obtained by solving Eqn. 7 numerically by discretization and iteratively. GVF is computed as a diffusion of the gradient vectors of an edge map derived from the image. The resultant field has a large capture range, which means that the active contour can be initialized far away from the desired boundary. The GVF field also tends to force active contours into boundary concavities, where traditional snakes have poor convergence. The GVF snakes converge to target boundaries and these boundaries segment the C-scan images to obtain a 3D Volumetric Segmented image. Examples of segmented volume are shown in Figs. 4 and 5. Fig. 4a shows the depth slices of preprocessed GPR data from 3D

Radar system. Two targets (simulated plastic mine and metal plate as reference) were buried in the sand whose signatures are indicated by arrows in the figure. 3D segmented image of Fig. 4a is shown in Fig. 4b. The segmented volume consists of two targets and a clutter. Fig. 5 shows another example for a simulated plastic mine buried in the soil. Data was collected using VNA based SFCW system in lab setup. 3D segmented image of the simulated mine is shown in the Fig. 5b. Features are extracted from the segmented volume for discrimination of targets form clutters as discussed in the following section.

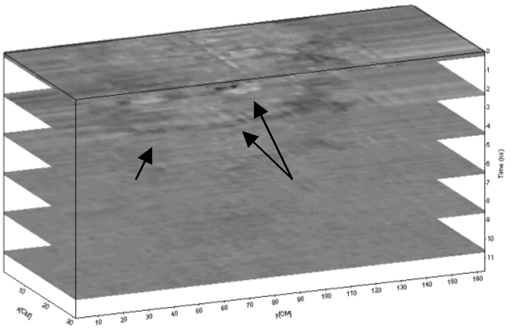

(a)

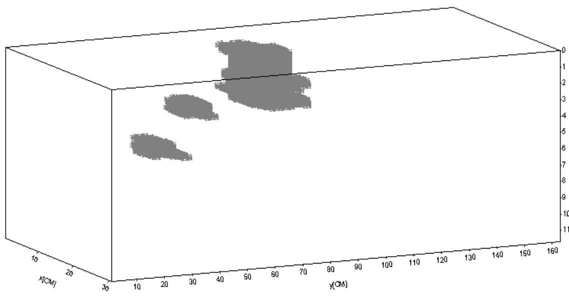

(b)

Figure 4. (a) Slices of time domain C-scan data (two targtes indicated by arrows) (b) 3D Segmented image of (a) using GVF snakes applied on volumes of ineterst identified by 3D LMS.

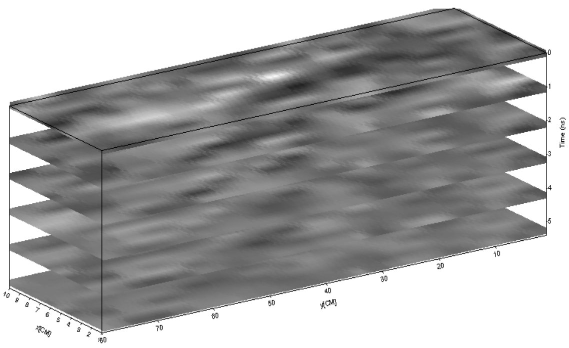

(a)

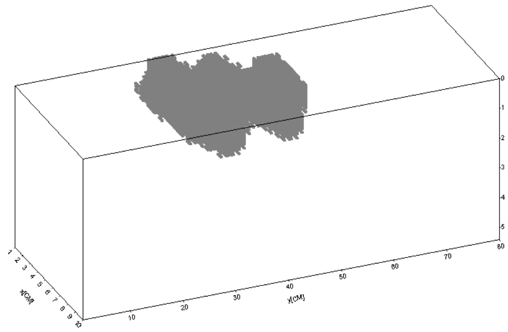

(b)

Figure 5. (a) Slices of time domain C-scan data (b) 3D Segmented image of (a) using GVF snakes applied on volumes of ineterst identified by 3D LMS.

D. Feature Extraction

After segmentation, ‘Solidity’ is computed for every segmented region and is used as feature for discriminating targets from clutters. Solidity is defined as ratio between area of the segmented region to the convex area of the region. Target is expected to have symmetrical shape, which gives a solid shape in the C-scan image. Whereas, clutter due to its irregular shape, has less solidity. The measure of solidity is then thresholded to identify the targets. Fig. 6 shows an example of discriminated targets obtained after feature extraction from Fig. 4b. The clutter which has irregular shape is discarded after the discrimination process. The performance of our proposed method is evaluated, which is presented in the following section.

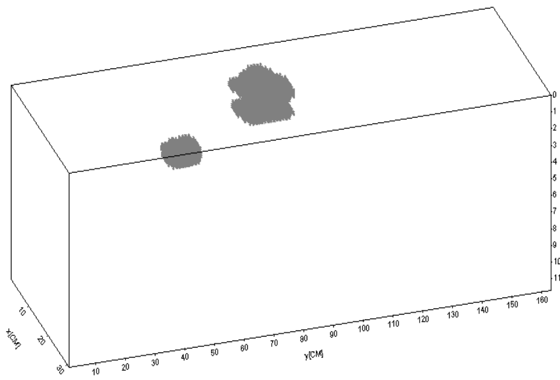

Figure 6. Discriminated targets after feature extraction from Fig. 4b.

III. EXPERIMENTAL RESULTS

Our algorithm was tested using the real-world data sets. Experiments were conducted on test bed using 3D Radar system. Number of targets used for our experiments were 43 and the types of the targets were metal plate and simulants of mine. Total lane area covered is 126 m2. Table 1 shows the test targets statistics. Burial depth of the targets varies from 10 cm to 25 cm.

TABLE I. TEST TARGETS STATISTIC

Types of soil	No. of targets
Sand	18
Silt	20
Clay	5
Total	43

The performance of our algorithm is measured using receiver operating characteristics, which is probability of detection versus false alarm rate. Probability of detection is defined as the ratio between number of correctly detected targets and total number of targets. False alarm rate is defined as the ratio between number of false alarms and total number of clutters. The measure of solidity gives the confidence value for the presence of targets. Our proposed algorithm is compared with anomaly detection algorithms: 3D LMS [3], 2D LMS algorithm [15] and Kalman filtering technique [19] for landmine detection. The detected output is said to be correct if it lies within 10 pixels from the center of the target. 2D LMS and Kalman Filtering algorithm gives detections in x and y locations. Hence to compare with these algorithms the detected x and y locations are used for validation. Depth information is not taken for comparison purpose.

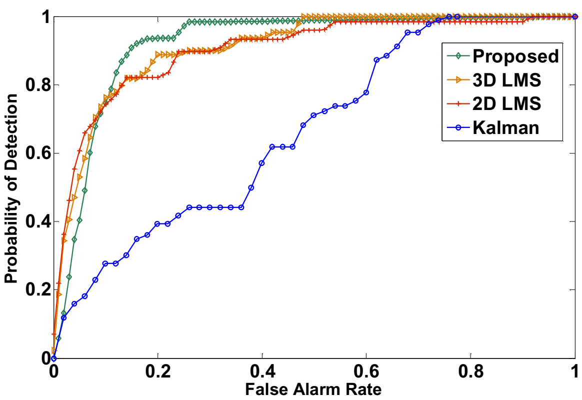

Figure 7. ROC Curve for 3D LMS, 2D LMS and Kalman Filtering.

Fig. 7 shows the ROC curve for the algorithms: Proposed discrimination algorithm, 3D LMS, 2D LMS and Kalman filtering. In terms of the area under the ROC curve, Kalman filtering is inferior to other algorithms, as it is more sensitive to the inhomogenieties in the soil. 2D LMS has shown a good performance and 3D LMS is superior to 2D LMS. Our proposed discrimination algorithm has reduced the false alarm rate of 3D LMS, for higher probability of detection.

IV. CONCLUSION

We have proposed a 3D image analysis method for landmine detection from GPR images. 3D volume of GPR data is preprocessed to remove ground bounce, antenna leakage and noise. 3D Adaptive filtering technique is used to detect anomalies in the volume. Gradient vector flow based image segmentation algorithm is used to get a 3D volumetric segmented image. Solidity of the segmented regions is used to discriminate targets from clutters. Our proposed method has shown improvement over other detection algorithms and has reduced the false alarm rate of the anomaly detection algorithms. The segmentation algorithm can also be applied on migrated images to get a refined shape of the target.

ACKNOWLEDGMENT

We acknowledge the help extended by Shri Alok Mukherjee (Head Robotics) and his team, Research and Development Laboratory (R&DE), Pune, India for our data collection, using their test setup.

REFERENCES

[1] Guidebook on Detection Technologies and Systems for Humanitarian Demining, GICHD, Geneva, March 2006. ISBN 2-88487-045-8.

[2] D.J. Daniels, "Ground Penetrating Radar", Second Edition, Published by: The Institution of Electrical Engineers, London, United Kingdom, 2004.

[3] A. Dyana , K Chandrasekharan, CH Srinivas Rao and R. Kuloor, "3D – Least Mean Square Algorithm for Anomaly Detection in Ground Penetrating Radar", International Radar Symposium India (IRSI 2011), Bangalore,India, December 2011.

[4] X. Feng, J. Fujiwara, Z. Zhou, T. Kobayashi and M. Sato, "Imaging algorithm of a Hand-held GPR MD sensor(ALIS)", Proc. Detection and remediation technologies for mines and minelike targets X, Volume 5794, 2005.

[5] P.D. Gader, J. Keller and B. Nelson, "Recognition technology for the detection of buried land mines", IEEE Transactions on Fuzzy Systems, vol. 9, no. 1, pp 31-43, February 2001.

[6] K. Ho and P. Gader, "A linear prediction land mine detection algorithm for hand held ground penetrating radar", IEEE Transactions of Geoscience and Remote Sensing, vol. 40, no. 6, pp. 963–976, June 2002.

[7] I. Bankman, "Handbook of Medical Imaging", Academic Press, September 2000.

[8] H. M. Jol., "Ground Penetrating Radar: Theory and Principles", First edition, Elsevier Publications, 2009.

[9] M. Kass, A. Witkin, and D. Terzopoulos, "Snakes: Active contour models," International Journal of Computer Vision, vol. 1, no. 4, pp. 321–331, Jan. 1987.

[10] N. William, C. T. Chan Thomas, H. C. So, and K. C. Ho, "Particle Filtering Based Approach for Landmine Detection Using Ground Penetrating Radar", IEEE Transactions on Geoscience and remote Sensing, vol. 46, no. 11, pp 3739-3755, November 2008.

[11] A. Peter Torrione, S. Chandra Throckmorton and M. Leslie Collins, "Performance of an Adaptive Feature-Based Processor for a Wideband Ground Penetrating Radar System", IEEE Transactions on Aerospace and Electronic Systems, vol. 42, no. 2, pp 644-658, April 2006.

[12] D. Potin, P. Vanheeghe, E. Duflos and M. Davy, "An abrupt change detection algorithm for buried landmines localization", IEEE Transactions on Geoscience and Remote Sensing, vol. 44, no. 2, pp. 260–272, June 2006..

[13] S. Tjora, E. Eide and L. Lundheim, "Evaluation of Methods for Ground Bounce Removal in GPR Utility Mapping", Tenth International Conference on Ground Penetrating Radar, Delft, The Netherlands, June, 2004.

[14] S. Haykin and B. Widrow, "Least Mean Square Adaptive Filters", Wiley InterScience, 2003.

[15] T. Soni, R. J. Zeidler and H. Walter Ku, "Performance Evaluation of 2-D Adaptive Prediction Filters for Detection of Small Objects in Image Data", IEEE Transactions on Image Processing, vol. 2, no. 3, pp 327-340, July1993.

[16] N. V. Verdenskaya, V.V. Sazonov, I.A. IvanovaI, A.G. Yarovoy and L.P. Ligthart, "Segmentation of GPR Images", Proceedings of the 3rd European Radar Conference, September 2006, pp 45-48.

[17] C. Xu and J. L. Prince, "Snakes, shapes, and gradient vector flow.", IEEE Transactions on Image Processing, vol. 7, no. 3, pp. 359–369, March 1998.

[18] L. Xu, E. Oja and P. Kutltanen, "A new curve detection method: randomized Hough Transform (RHT)", Pattern Recognition Letters, Vol. 11, No. 5, pp. 331–338, May 1990.

[19] A. Zoubir, I. Chant, C. Brown, B. Barkat and C. Abeynayake, "Signal processing techniques for landmine detection using impulse ground penetrating radar", IEEE Sensors Journal, vol. 2, no. 1, pp. 41–51, February 2002.